Preprints, 4th IFAC Conference on
Advances in Proportional-Integral-Derivative Control
Almería, Spain | June 12-14, 2024

Utopian robust efficiency indicator for robust PID multi-objective tunning ⋆

Uriel Veyna * **Xavier Blasco** * **Juan Manuel Herrero** *
Alberto Pajares *

* *Instituto Universitario de Automática e Informática Industrial. Universitat Politècnica de València, Valencia 46022, Spain; (e-mail: {urveyro1, xblasco, juaherdu, alpafer1}@upv.es).*

Abstract: This paper describes the robust design of a multi-loop PID temperature control of a PEMFC stack. A multi-objective optimization approach is used, considering uncertainties in the dynamic model parameters. A new quality indicator in the optimization process, utopian robust efficiency, is defined for tuning PID parameters. To compare this approach, the alternative designs based on optimizing the worst case and the system performance in the nominal model are aborded. The results show that the controllers tuned based on the utopian robust efficiency exhibit a better trade-off between optimal performance in the nominal model and robustness in the presence of uncertainty.

Keywords: Identification methods for PID control design.; PID control performance assessment.; Applications of PID control.

1. INTRODUCTION

As a solution to environmental problems such as global warming, air pollution, and depletion of fossil fuel reserves, there is growing interest in using fuel cell-based systems. One of the possible fields of application is the use of micro combined heat and power system (micro-CHP). These systems produce electricity and heat (cogeneration) for energy supply in the residential sector (Ellamla et al., 2015). Due to their high electrical efficiency, the Proton Exchange Membrane Fuel Cell (PEMFC) stack can be the prime mover of a micro-CHP. The main advantage of these systems is the use of the thermal energy produced as a result of electricity generation that increases the overall performance of the system (Navarro Giménez et al., 2019). The electrical efficiency, lifetime of the stack, and overall efficiency of the micro-CHP system depend on proper temperature control. For correct operation, the stack temperature must be maintained within defined limits. A cooling system is used to cool the stack and keep its temperature at its optimum value. The stack's durability, cost, reliability, and energy efficiency largely depend on the correct design of this cooling control system.

For nonlinear systems, it is useful to design controllers using optimization techniques. The design of the temperature control of a PEMFC stack involves more than a single objective: the temperature gradient of the stack and control efforts. Previous works (Pajares et al., 2020b; Navarro et al., 2020; Navarro Giménez et al., 2019) address this problem by formulating a multi-objective optimization problem using a nominal parameter model (without considering uncertainties). However, in real applications, system parameters are subject to variations and uncertainties. It has been shown that even a slight modification of parameters in an optimization problem can cause drastic effects on the optimal solutions obtained, resulting in suboptimality or infeasibility (Shang et al., 2017).

To formulate a robust control optimization problem that aims to achieve an appropriate system response despite parameter variations, two key elements must be considered. These elements are the definition of a framework of uncertainty scenarios and establishing robust indicators that evaluate the sensitivity of the resulting solutions. Defining a set of scenarios that adequately represents the uncertainties of the analysis problem is a complex task. Some of the most relevant criteria to be considered in this process are discussed in (Shang et al., 2017). An appropriate uncertainty modeling should exclude scenarios of variations with a low probability of existence that lead to determining over-conservative solutions in the decision-making stage. Furthermore, the number of scenarios must be sufficient to describe the possible space of variations correctly but not too large for the computational cost of the sensitivity analysis to be unaffordable. Traditionally, formulating an optimization problem under uncertainties involves the establishment of quality indicators that condition the identification of solutions to specific robustness criteria or design constraints. The Minmax robust indicator is described in papers such as (Veyna et al., 2023b). This index is often used to minimize the worst-case assessment of each component of the objective vector when evaluating a set of uncertainty scenarios. Other indicators used are the mean and standard deviation. In papers like (Paenke et al., 2006), these variance estimators are used

⋆ This work was supported in part by the grant PID2021-124908NB-I00 founded by MCIN/AEI/10.13039/50110001 1033/ and by "ERDF A way of making Europe"; by grant PRE2019-087579 funded by MCIN/AEI/ 10.13039/501100 011033 and by "ESF Investing in your future"; and by the Generalitat Valenciana regional government through project CIAICO/2021/064.

to formulate the minimization function in different test problems under a multi-objective approach.

In the context of a robust optimization problem, the optimality for the nominal process and robustness in the presence of uncertainty are usually in conflict (Gaspar-Cunha and Covas, 2008). If it is desired to address the problem based on a nominal scenario, the solutions obtained are usually less robust for the rest of the scenarios. On the other hand, if it is desired to minimize the variance concerning a set of uncertainty scenarios, the performance of the solutions obtained under the nominal scenario may be far from optimality. Based on this problem, a new robustness indicator called utopian robust efficiency is proposed in this paper. With this indicator, we seek to define controllers with a trade-off between optimality and robustness. In this work, we apply the methodology for tuning a multi-loop PID control structure to control the temperatures of a PEMFC system with model uncertainties. Afterward, to compare and highlight the properties and advantages obtained from the tuned controllers based on this indicator, we also address the alternative optimization problems associated with performance in the nominal parameter model and the Minmax robust indicator.

2. MULTI-OBJECTIVE OPTIMIZATION PROBLEMS UNDER UNCERTAINTIES

The classical approach of a multi-objective optimization problem aims to optimize a cost function composed of objectives that are usually in conflict. When considering an approach under uncertainties, the formulation of the problem becomes more complex, and the definition of a solution is less trivial. To properly adjust the level of robustness in a solution, two key elements are required: 1) a set of scenarios that adequately represent the uncertainties of the system and 2) indicators that evaluate the quality of robustness in the defined solutions.

2.1 Formulation of uncertainty frameworks

Under an optimization problem, uncertainty can be modeled as slight variations associated with the parameters of the objective function (Paenke et al., 2006). A multi-objective function $\boldsymbol{f(x,p)} \in \boldsymbol{W}$ can be defined as $\boldsymbol{f(x,p)} = [f_1(\boldsymbol{x},\boldsymbol{p}), f_2(\boldsymbol{x},\boldsymbol{p}), ..., f_q(\boldsymbol{x},\boldsymbol{p})]$, where $q \in \mathbb{N}$ is the number of objectives. A decision vector $\boldsymbol{x} \in \boldsymbol{Q}$ can be defined as $\boldsymbol{x} = [x_1, x_2, ..., x_h]$, where $h \in \mathbb{N}$ is the number of decision variables. An uncertainty parameter model $\boldsymbol{p}$ is defined as $\boldsymbol{p} = [p_1, p_2, ..., p_k]$, where $k \in \mathbb{N}$ is the number of parameters where variations are considered. Properly defining an uncertainty framework $\boldsymbol{P} = \{\boldsymbol{p}^1, \boldsymbol{p}^2, ..., \boldsymbol{p}^m\}$, $m \in \mathbb{N}$ in real engineering applications must constitute a set of highly representative scenarios $\boldsymbol{p} \in \boldsymbol{P}$ that face the system while representing a computationally feasible cost for robustness analyses (Veyna et al., 2023b).

2.2 Robust Pareto dominance concepts

To perform a robustness analysis, it is necessary to define appropriate qualitative indicators. These robust indicators evaluate the performance of a solution under uncertainties based on different concepts of Pareto dominance.

Definition 1. Pareto classical dominance (Miettinen, 2012): Given a scenario $\boldsymbol{p}$, a decision vector $\boldsymbol{x}^1$ is dominated by another decision vector $\boldsymbol{x}^2$ if, $f_i(\boldsymbol{x}^2, \boldsymbol{p}) \leq f_i(\boldsymbol{x}^1, \boldsymbol{p})$ for all $i \in [1, 2, ..., q]$ and $f_j(\boldsymbol{x}^2, \boldsymbol{p}) < f_j(\boldsymbol{x}^1, \boldsymbol{p})$ for at least one j such that $j \in [1, 2, \ldots, q]$.

The Pareto dominance between vectors $\boldsymbol{x} \in \boldsymbol{Q}$ in scenario $\boldsymbol{p}$ is denoted as $\boldsymbol{x}^2 \preceq^p \boldsymbol{x}^1$. Conversely, the non-dominance between vectors is denoted as $\boldsymbol{x}^2 \npreceq^p \boldsymbol{x}^1$. The set of Pareto solutions in scenario $\boldsymbol{p}$ is denoted as $\boldsymbol{X}^p = \{\boldsymbol{x} \in \boldsymbol{Q} | \nexists \boldsymbol{x}^0 \in \boldsymbol{Q} : \boldsymbol{x}^0 \preceq^p \boldsymbol{x}\}$. Then, the set of uncertainty scenarios $\boldsymbol{P} = \{\boldsymbol{p}^1, \boldsymbol{p}^2, ..., \boldsymbol{p}^m\}$, $m \in \mathbb{N}$ defines the family of Pareto sets $\{\boldsymbol{X}^{\boldsymbol{p}^1}, \boldsymbol{X}^{\boldsymbol{p}^2}, ..., \boldsymbol{X}^{\boldsymbol{p}^m}\}$.

Definition 2. Robust dominance (Veyna et al., 2023a): Given a set of scenarios $\boldsymbol{P} = \{\boldsymbol{p}^1, \boldsymbol{p}^2, ..., \boldsymbol{p}^m\}$, a decision vector $\boldsymbol{x}^1$ is robustly dominated by another decision vector $\boldsymbol{x}^2$ if the classical dominance $\boldsymbol{x}^2 \preceq^{p^s} \boldsymbol{x}^1$ is satisfied for all $s \in [1, 2, ..., m]$.

The robust dominance between vectors is denoted as $\boldsymbol{x}^2 \preceq^P \boldsymbol{x}^1$. On the other hand, the non-robust dominance is indicated as $\boldsymbol{x}^2 \npreceq^P \boldsymbol{x}^1$.

Definition 3. Point-based Minmax robust efficiency (Ide and Schöbel, 2016): given a set of uncertainty scenarios $\boldsymbol{P} = \{\boldsymbol{p}^1, \boldsymbol{p}^2, ..., \boldsymbol{p}^m\}$, the Point-based Minmax efficiency of vector $\boldsymbol{x} \in \boldsymbol{Q}$ is defined by the function $\boldsymbol{f^{max}(x,P)} = [f_1^{max}(\boldsymbol{x},\boldsymbol{P}), f_2^{max}(\boldsymbol{x},\boldsymbol{P}), ..., f_q^{max}(\boldsymbol{x},\boldsymbol{P})]$. Where the component $f_i^{max}(\boldsymbol{x},\boldsymbol{P})$ such that $i \in [1, 2, ..., q]$ is defined as $f_i^{max}(x, P) = \max_{\boldsymbol{p} \in \boldsymbol{P}} \boldsymbol{f_i(x,p)}$.

The function $\boldsymbol{f^{max}(x,P)}$ determines the maximum value reached by a solution $\boldsymbol{x}$ under $\boldsymbol{P}$ in each f_i such that $i \in [1, 2, ..., q]$. Based on this indicator, Point-based Minmax dominance between vectors $\boldsymbol{x} \in \boldsymbol{Q}$ is stated as follows:

Definition 4. Point-based Minmax robust dominance. Given a set of uncertainty scenarios $\boldsymbol{P} = \{\boldsymbol{p}^1, \boldsymbol{p}^2, ..., \boldsymbol{p}^m\}$, a decision vector $\boldsymbol{x} \in \boldsymbol{Q}$ is dominated by another vector $\boldsymbol{x}^0 \in \boldsymbol{Q}$ under the Point-based Minmax robust concept (denoted as $\boldsymbol{x}^0 \preceq^{max} \boldsymbol{x}$) if any of the following conditions are satisfied:

Condition 1:$\boldsymbol{f^{max}(x,P) = f^{max}(x^0,P)}$:

$\boldsymbol{x}^0 \preceq^{max} \boldsymbol{x}$ if $\boldsymbol{x}^0 \preceq^P \boldsymbol{x}$.

Condition 2:$\boldsymbol{f^{max}(x,P) \neq f^{max}(x^0,P)}$:

$\boldsymbol{x}^0 \preceq^{max} \boldsymbol{x}$ if $f_i^{max}(\boldsymbol{x}^0, \boldsymbol{P}) \leq f_i^{max}(\boldsymbol{x}, \boldsymbol{P})$ for all $i \in [1, 2, ..., q]$ and $f_j^{max}(\boldsymbol{x}^0, \boldsymbol{P}) < f_j^{max}(\boldsymbol{x}, \boldsymbol{P})$ for at least one $j \in [1, 2, ..., q]$.

Under Point-based Minmax dominance concept, the non-dominated solutions constitute the Point-based Minmax robust set $\boldsymbol{X^{Wc}} = \{\boldsymbol{x} \in \boldsymbol{Q} | \nexists \boldsymbol{x}^0 \in \boldsymbol{Q} : \boldsymbol{x}^0 \preceq^{max} \boldsymbol{x}\}$.

In order to define solutions with a balanced performance for the whole uncertainty framework, we highlight the utopian robust efficiency indicator (Definition 5). This new indicator is proposed to evaluate the global deviation of a solution's performance under uncertainties concerning the utopian points defined from the classical optimization problem for each scenario $\boldsymbol{p} \in \boldsymbol{P}$. With this indicator, we seek to tune controllers with a good trade-off between robustness and optimality.

Definition 5. Utopian robust efficiency (Veyna et al., 2023a): given a set of scenarios $\boldsymbol{P} = \{\boldsymbol{p}^1, \boldsymbol{p}^2, ..., \boldsymbol{p}^m\}$, the function $\boldsymbol{f^{ut}(x, P)} = [f_1^{ut}(\boldsymbol{x}, \boldsymbol{P}), f_2^{ut}(\boldsymbol{x}, \boldsymbol{P}), ..., f_q^{ut}(\boldsymbol{x}, \boldsymbol{P})]$ defines the utopian robust efficiency of a vector $\boldsymbol{x}$. Where the element $f_i^{ut}(\boldsymbol{x}, \boldsymbol{P})$ such that $i \in [1, 2, ..., q]$ is defined as given in equations (1)-(2).

$$f_i^{ut}(\boldsymbol{x}, \boldsymbol{P}) = \sum_{s=1}^{m} \Delta f_i(\boldsymbol{x}, \boldsymbol{p}^s) \quad (1)$$

$$\Delta f_i(\boldsymbol{x}, \boldsymbol{p}^s) = \frac{f_i(\boldsymbol{x}, \boldsymbol{p}^s) - \min(f_i(\boldsymbol{X}^{p^s}, \boldsymbol{p}^s))}{\max(f_i(\boldsymbol{X}^{p^s}, \boldsymbol{p}^s)) - \min(f_i(\boldsymbol{X}^{p^s}, \boldsymbol{p}^s))} \quad (2)$$

The function $\boldsymbol{f^{ut}(x, P)}$ defines a normalized measure for the global deviation of the objective function under uncertainties $f_i^{ut}(\boldsymbol{x}, \boldsymbol{P}) = [f_i^{ut}(\boldsymbol{x}, \boldsymbol{p^1}), f_i^{ut}(\boldsymbol{x}, \boldsymbol{p^2}), ..., f_i^{ut}(\boldsymbol{x}, \boldsymbol{p^m})]$ concerning the utopian points $\min(\boldsymbol{f_i(X^{p^s}, p^s)})$, $s \in [1, 2, ..., m]$ determined for each scenario. Figure 1 shows a graphical example in 2 dimensions ($i \in [1, 2]$) where the parameters of function $\Delta f_i(\boldsymbol{x}, \boldsymbol{p}^s)$ for any scenario $\boldsymbol{p}^s$, $s \in [0, 1, ..., m]$ are indicated.

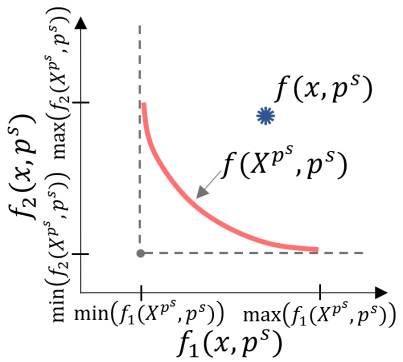

Fig. 1. Parameters of function $\Delta f_i(\boldsymbol{x}, \boldsymbol{p}^s)$ in 2 dimensions for any scenario $\boldsymbol{p}^s$, $s \in [0, 1, ..., m]$.

Definition 6. Utopian robust dominance: given a set of scenarios $\boldsymbol{P} = \{\boldsymbol{p}^1, \boldsymbol{p}^2, ..., \boldsymbol{p}^m\}$, a decision vector $\boldsymbol{x} \in \boldsymbol{Q}$ is dominated under the utopian robust concept by another decision vector $\boldsymbol{x}^0$ (denoted as $\boldsymbol{x}^0 \preceq^{ut} \boldsymbol{x}$) if $f_i^{ut}(\boldsymbol{x}^0, \boldsymbol{P}) \leq f_i^{ut}(\boldsymbol{x}, \boldsymbol{P})$ for all $i \in [1, 2, ..., q]$ and $f_j^{ut}(\boldsymbol{x}^0, \boldsymbol{P}) < f_j^{ut}(\boldsymbol{x}, \boldsymbol{P})$ for at least one $j \in [1, 2, ..., q]$.

Under utopian robust dominance, the non-dominated solutions constitute the Utopian robust set $\boldsymbol{X^{Ut}} = \{\boldsymbol{x} \in \boldsymbol{Q} | \nexists \boldsymbol{x}^0 \in Q : \boldsymbol{x}^0 \preceq^{ut} \boldsymbol{x}\}$ that stands out for representing a balanced performance under all uncertainty scenarios (Veyna et al., 2023a).

3. SYSTEM DESCRIPTION AND CONTROL PROBLEM FORMULATION

3.1 PEM system description

The PEMFC stack that is located in our laboratory, is supplied with hydrogen and air to generate electrical energy and heat. A programmable electronic load is used to emulate a residential consumption of electricity (electrical appliances). A radiator simulates the heat energy consumption (hot water and heating) by extracting heat when activated. Additionally, thermal energy can be stored in a water tank. Details of the description of this system can be found in (Navarro Giménez et al., 2019).

For the PEMFC stack temperature control design, a model of the cooling circuit of the micro-CHP system is used. Figure 2 shows a black box diagram of the model detailed in (Navarro et al., 2020). The model has two outputs related to the liquid coolant: the stack water outlet and inlet temperatures $T_{w_{out}}$ and $T_{w_{in}}$. The control actions are $u_{T_{wout}}$, which represents the water flow rate in the primary cooling circuit, and $u_{T_{win}}$, which is the water flow rate in the secondary cooling circuit. The only disturbance considered is the electric current (I) demanded by the stack. This nonlinear model is built from first principles and was experimentally validated with a wide operating range (from 140 to 200A).

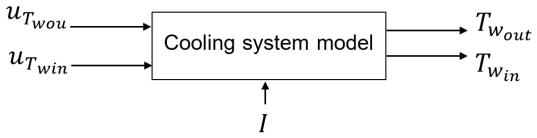

Fig. 2. Black box diagram of the model.

This dynamic model have 31 parameters $\boldsymbol{p} = [p_1, p_2, ..., p_{31}]$. In (Navarro Giménez et al., 2019), details of the parameter identification and validation of a nominal model for the cooling system can be found. In (Pajares et al., 2020a), near-optimal models are analyzed, and an approximation of the operating ranges for the parameter uncertainties when the system operates around its set point is presented.

3.2 Uncertainty modelling

The methodology used to address the design problem for modeling the parameter uncertainties of this system has been presented in a previous work (Veyna et al., 2023b). The result is a set of uncertainty models that represent highly probable occurrence scenarios, limiting the degree of conservatism and representing an adequate computational cost to address the optimization process. Before applying this methodology, the following initial elements were considered:

(1) The nominal parameter model. From the identification process (Navarro Giménez et al., 2019), the nominal model of parameters $\boldsymbol{p}^0 = [p_1^0, p_2^0, ..., p_{31}^0]$ is defined (Values are reported in (Veyna et al., 2023b)).
(2) Degradation limit for system response. From the validation process, an average temperature error $J_{avg} = 0.26°C$ is associated with the identified nominal model (see the model validation test in (Navarro Giménez et al., 2019)). On the basis of this data, the temperature degradation limit of $0.65°C$ is established as a degree of tolerance for the classification of uncertainty models with acceptable reliability.
(3) Initial ranges of variation for each parameter. The scanning ranges $[\underline{pp_i}, \overline{pp_i}]$, $i = [1, 2, ..., 31]$ on which the domain of uncertainty is initially explored are defined by the deviation of $\pm 95\%$ from the nominal value of each parameter. From these ranges, as described in (Veyna et al., 2023b), a series of sensitivity analyses will lead to establishing more appropriate limits for the parameter uncertainty domain based on conservatism criteria.

After applying this uncertainty modeling methodology, the set of models $\boldsymbol{P}^{\alpha} = \{\boldsymbol{p}^1, \boldsymbol{p}^2, ..., \boldsymbol{p}^{145}\}$ is defined. Figure 3

shows an overview of this modeling process. Where given a model $\boldsymbol{p} \in \boldsymbol{P}^{\alpha}$, the function $f_e(e_m)$ is an indicator that evaluates the error between the model output and the measured system response in an open-loop experiment. $\gamma(\boldsymbol{p})$ is an indicator that evaluates the global relative deviation from the nominal model in the parameter space. Both indicators are described in (Veyna et al., 2023b).

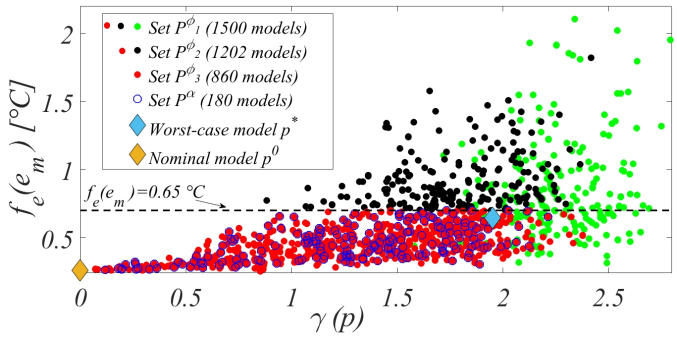

Fig. 3. Overview of the uncertainty modeling process for the PEMFC system

At first, the uncertainty modeling process begins with the set of models $\boldsymbol{P}^{\phi_1} = \{\boldsymbol{p}^1, \boldsymbol{p}^2, ..., \boldsymbol{p}^{1500}\}$, which is defined with 1500 models (green, black, and red dots) created by random sampling within the operating range established in the sensitivity analysis. Then, three filters are applied to simplify the set of models. By applying the first filter, improbable models concerning variations in parameter space are excluded, and the subset $\boldsymbol{P}^{\phi_2} \subset \boldsymbol{P}^{\phi_1}$ of 1202 models (black and red dots) is defined. By applying the second filter, the subset $\boldsymbol{P}^{\phi_3} \subset \boldsymbol{P}^{\phi_2}$ of 860 models (red dots) is obtained by simplification concerning the model's performance and the constraint fixed $f_e(e_m) < 0.65°C$. The last filter is used to uniformly simplify the modeling to a computationally acceptable representation for evaluating the sensitivity of a solution in a robustness analysis. We defined the subset $\boldsymbol{P}^{\alpha} \subset \boldsymbol{P}^{\phi_3}$ (blue circles) with 180 models. Finally, using the model selection strategy defined in stage 3 of the methodology described in (Veyna et al., 2023b), the worst-case model $\boldsymbol{p}^* \in \boldsymbol{P}^{\alpha}$ is identified. This model selection strategy consists of using a set of reference controllers to characterize the performance of the uncertainty set $\mathbf{P}^{\alpha}$ in the objective space. In figure 3, the nominal model $\boldsymbol{p}^0$ is represented by a yellow diamond. A blue diamond represents the worst-case model $\boldsymbol{p}^*$.

3.3 Temperature control problem formulation

The control system aims to keep $T_{w_{out}}$ and $T_{w_{in}}$ at their corresponding setpoints while changes in the electrical current demand (I) produce undesirable transient fluctuations in the stack temperature. The temperature control must respond to disturbances to minimize the excursions of $T_{w_{out}}$ and $T_{w_{in}}$ from their setpoints, $r_{T_{wout}} = 65°C$ and $r_{T_{in}} = 60°C$, respectively. In (Navarro et al., 2020) is proposed a multi-loop control structure (see figure 4); this structure consists of two PI controllers with anti-windup, one for the control of $T_{w_{out}}$ (by using $u_{T_{wout}}$) and the other for the control of $T_{w_{in}}$(by using $u_{T_{win}}$). Therefore, the controller has four parameters to adjust (two for each PI), $[K_{c1}, T_{i1}, K_{c2}, T_{i2}]$, where K_{c1} and K_{c2} are in ((l/min)/°C)

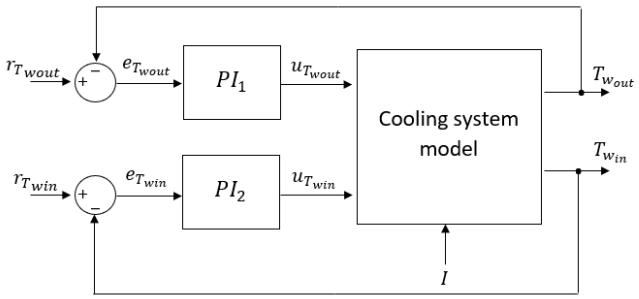

Fig. 4. Multi-loop PI control structure for temperatures T_{wout} and T_{win}.

and T_{i1} and T_{i2} in (s). The formulation of the multi-objective optimization problem under uncertainties aims to minimize the objectives f_1 and f_2 stated in equations (3) and (4).

$$f_1(\boldsymbol{x}, \boldsymbol{p}) = \frac{1}{T_{sim}} \int_0^{T_{sim}} |e_{T_{w_{out}}}| dt + \frac{1}{T_{sim}} \int_0^{T_{sim}} |e_{T_{w_{in}}}| dt \quad (3)$$

$$f_2(\boldsymbol{x}, \boldsymbol{p}) = \frac{1}{T_{sim}} \int_0^{T_{sim}} \left| \frac{du_{T_{w_{out}}}(t)}{dt} \right| dt + \frac{1}{T_{sim}} \int_0^{T_{sim}} \left| \frac{du_{T_{w_{in}}}(t)}{dt} \right| dt \quad (4)$$

Where $\boldsymbol{p} = [p_1, p_2, ..., p_k]$ is the vector of model parameters and $\boldsymbol{x} = [K_{c1}, T_{i1}, K_{c2}, T_{i2}]$ is the decision vector (containing the controller parameters). The lower and upper bounds for controller tuning are $\underline{\boldsymbol{x}} = [\underline{K_{c1}}, \underline{T_{i1}}, \underline{K_{c2}}, \underline{T_{i2}}]$ and $\overline{\boldsymbol{x}} = [\overline{K_{c1}}, \overline{T_{i1}}, \overline{K_{c2}}, \overline{T_{i2}}]$. Objective $f_1(\boldsymbol{x}, \boldsymbol{p})$ evaluates the performance of the controllers by adding the mean absolute errors of the stack output and input temperatures (in °C) concerning their setpoints (equation (5)).

$$e_{T_{w_{out}}} = r_{T_{w_{out}}} - T_{w_{out}};\ e_{T_{w_{in}}} = r_{T_{w_{in}}} - T_{w_{in}} \quad (5)$$

Objective $f_2(\boldsymbol{x}, \boldsymbol{p})$ evaluates the control effort by adding the average absolute values of the rates of change of the control actions ($u_{T_{w_{out}}}$ and $u_{T_{w_{in}}}$) in $(l/min)/s$. T_{sim} is the simulation time (3300s).

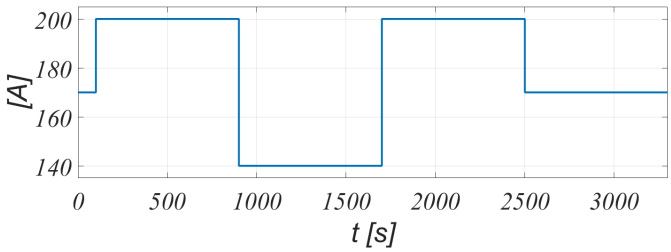

Fig. 5. Electric current demand signal used in the control design. The first step applied is at t=100s, and the span of each step is 800s. The total simulation time is 3300s.

These functions aim to achieve optimal electrical efficiency and minimal deterioration of the stack and actuators. In (Navarro et al., 2020), the temperature control design is addressed as a 4-objective optimization problem. To reduce the computational cost of the optimization process, this work simplifies the formulation and defines f_1 and f_2 as two aggregate objective functions that are combined with the same relevance. Temperature control should respond to changes in the current electricity demand. Figure 5 shows the electric current signal used for the con-

trol design that presents steps and traverses through the full validity range of the nonlinear model (from 140 to 200A). Given these conditions and the robustness indicators shown in section 2, the multi-objective optimization problem is stated under three formulations:

a) Under the function $\boldsymbol{f}(\boldsymbol{x}, \boldsymbol{p}^0)$

$$\min_{\boldsymbol{x}} \boldsymbol{f}(\boldsymbol{x}, \boldsymbol{p}^0) \tag{6}$$

$$\boldsymbol{f}(\boldsymbol{x}, \boldsymbol{p}^0) = [f_1(\boldsymbol{x}, \boldsymbol{p}^0), f_2(\boldsymbol{x}, \boldsymbol{p}^0)] \tag{7}$$

b) Under the Minmax robust indicator $\boldsymbol{f^{max}}(\boldsymbol{x}, \boldsymbol{P})$

$$\min_{\boldsymbol{x}} \boldsymbol{f^{max}}(\boldsymbol{x}, \boldsymbol{P^{\alpha}}) \tag{8}$$

$$\boldsymbol{f^{max}}(\boldsymbol{x}, \boldsymbol{P^{\alpha}}) = [\boldsymbol{f_1^{max}}(\boldsymbol{x}, \boldsymbol{P^{\alpha}}), \boldsymbol{f_2^{max}}(\boldsymbol{x}, \boldsymbol{P^{\alpha}})] \tag{9}$$

c) Under the Utopian robust indicator $\boldsymbol{f^{ut}}(\boldsymbol{x}, \boldsymbol{P})$

$$\min_{\boldsymbol{x}} \boldsymbol{f^{ut}}(\boldsymbol{x}, \boldsymbol{P^{\beta}}) \tag{10}$$

$$\boldsymbol{f^{ut}}(\boldsymbol{x}, \boldsymbol{P^{\beta}}) = [\boldsymbol{f_1^{ut}}(\boldsymbol{x}, \boldsymbol{P^{\beta}}), \boldsymbol{f_2^{ut}}(\boldsymbol{x}, \boldsymbol{P^{\beta}})] \tag{11}$$

Where $\boldsymbol{P}^{\alpha} = \{\boldsymbol{p}^1, \boldsymbol{p}^2, ..., \boldsymbol{p}^{180}\}$ is the set of models describing the global uncertainty framework of the system and $\boldsymbol{P}^{\beta} = \{\boldsymbol{p}^0, \boldsymbol{p}^*\}$ is the set formed by the nominal model and the worst-case model defined from applying stage 3 of the uncertainty modelling methodology. The formulations a), b) and c) are subjet to $\underline{\boldsymbol{x}} \leq \boldsymbol{x} \leq \overline{\boldsymbol{x}}$, such that the controller parameters $[K_{c1}, T_{i1}, K_{c2}, T_{i2}]$ are discretized with a period of $[0.001, 0.01, 0.001, 0.01]$ and the limits $[\underline{\boldsymbol{x}}, \overline{\boldsymbol{x}}]$ are established as $\underline{\boldsymbol{x}} = [-8, 1, -8, 1]$ and $\overline{\boldsymbol{x}} = [-0.1, 120, -0.1, 120]$.

4. ANALYSIS OF RESULTS

To address the multi-objective optimization problems formulated in equations (6)-(11), the evMOGA algorithm is used (Herrero et al., 2009), although any other multi-objective optimization algorithm could be used. After finishing the optimization process, 25800 evaluations of the objective function $f(\boldsymbol{x}, \boldsymbol{p})$ were performed to determine the set of controllers $\boldsymbol{X^{Nom}}$, $\boldsymbol{X^{Wc}}$ and $\boldsymbol{X^{Ut}}$. In this process, the multi-objective optimization strategy presented in (Veyna et al., 2023a) was used to obtain all these sets simultaneously under a single run of the optimizer. The amounts of controllers that compose each of these sets are: $\#\boldsymbol{X^{Nom}} = 31$, $\#\boldsymbol{X^{Wc}} = 47$ and $\#\boldsymbol{X^{Ut}} = 56$. To compare the optimal and robust performance of these controller sets, figures 6 and 7 show the analysis under the functions $\boldsymbol{f^{ut}}(\boldsymbol{x}, \boldsymbol{P^{\beta}})$, $\boldsymbol{f^{max}}(\boldsymbol{x}, \boldsymbol{P^{\alpha}})$ and $\boldsymbol{f}(\boldsymbol{x}, \boldsymbol{p^0})$. Under function $\boldsymbol{f^{ut}}(\boldsymbol{x}, \boldsymbol{P^{\beta}})$, which evaluates the balance of performance between the nominal scenario $\boldsymbol{p}^0$ and the worst-case scenario $\boldsymbol{p}^*$, figure 6 shows that controllers $\boldsymbol{X}^{Ut}$ (green diamonds) belong to the optimization front $\boldsymbol{f^{ut}}(\boldsymbol{X^{Ut}}, \boldsymbol{P^{\beta}})$ defined from the utopian robust concept. Under this same indicator, some solutions $\boldsymbol{x} \in \boldsymbol{X}^{Nom}$ (red asterisks) and $\boldsymbol{x} \in \boldsymbol{X}^{Wc}$ (black squares) represent sub-optimal controllers and others belong to the optimization front. This figure highlights three reference controllers: $\boldsymbol{x}^3 \in \boldsymbol{X}^{Ut}$ (solid green circle), $\boldsymbol{x}^2 \in \boldsymbol{X}^{Wc}$ (solid black circle), and $\boldsymbol{x}^1 \in \boldsymbol{X}^{Nom}$ (solid red circle). These controllers are selected to represent a balanced performance of objectives concerning each of the optimization fronts $f^{ut}(\boldsymbol{X^{Ut}}, \boldsymbol{P^{\beta}})$, $f^{max}(\boldsymbol{X^{Wc}}, \boldsymbol{P^{\alpha}})$ and $f(\boldsymbol{X^{Nom}}, \boldsymbol{p}^0)$ respectively. Figure 7 shows the performance of sets $\boldsymbol{X^{Ut}}$, $\boldsymbol{X^{Wc}}$ and $\boldsymbol{X}^{Nom}$ in the objective space $[f_1(\boldsymbol{x}, \boldsymbol{p}), f_2(\boldsymbol{x}, \boldsymbol{p})]$ under the functions $f(\boldsymbol{x}, \boldsymbol{p}^0)$ and $\boldsymbol{f^{max}}(\boldsymbol{x}, \boldsymbol{P^{\alpha}})$. Red crosses and asterisks represent the controllers $\boldsymbol{x} \in \boldsymbol{X}^{Nom}$, circles and squares in black indicate the controllers $\boldsymbol{x} \in \boldsymbol{X}^{Wc}$, and green triangles and diamonds represent the controllers $\boldsymbol{x} \in \boldsymbol{X}^{Ut}$.

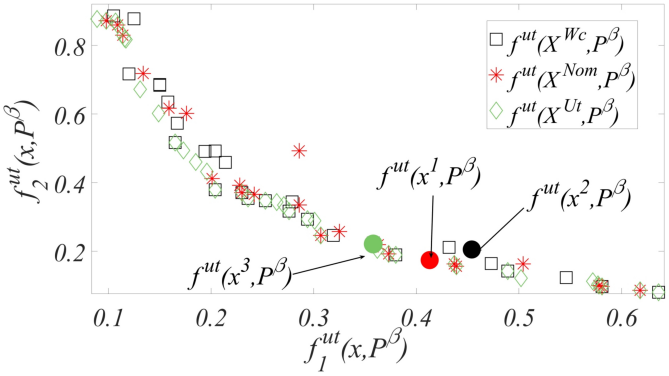

Fig. 6. Performance of controllers $\boldsymbol{X^{Nom}}$, $\boldsymbol{X^{Wc}}$, and $\boldsymbol{X^{Ut}}$ under the function $f^{ut}(\boldsymbol{x}, \boldsymbol{P}^{\alpha})$.

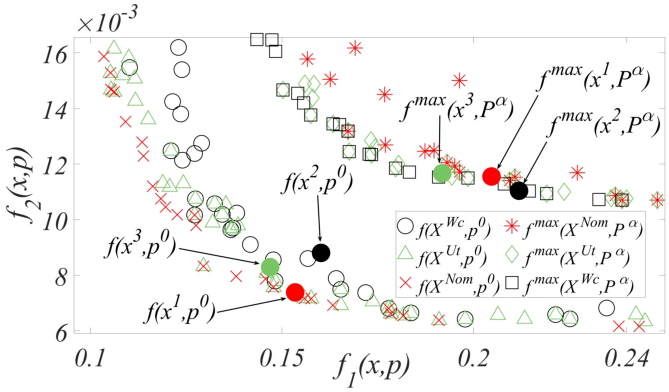

Fig. 7. Performance of controllers $\boldsymbol{X^{Nom}}$, $\boldsymbol{X^{Wc}}$, and $\boldsymbol{X^{Ut}}$ under the functions $f(\boldsymbol{x}, \boldsymbol{p}^0)$ and $f^{max}(\boldsymbol{x}, \boldsymbol{P}^{\alpha})$.

This figure evidences the conflict between controllers $\boldsymbol{X}^{Nom}$, which seeks the optimal performance in the nominal scenario $\boldsymbol{p^0}$, and controllers $\boldsymbol{X}^{Wc}$, which aims to minimize the Minmax robust indicator $f^{max}(\boldsymbol{x}, \boldsymbol{P^{\alpha}})$ under the uncertainty framework $\boldsymbol{P}^{\alpha}$. In this context, the set of controllers $\boldsymbol{X}^{Ut}$ tends to show a balance between both performance indicators. There are solutions $\boldsymbol{x} \in \boldsymbol{X}^{Nom}$ and $\boldsymbol{x} \in \boldsymbol{X}^{Wc}$ that also belong to the optimization front $f^{ut}(\boldsymbol{X^{Ut}}, \boldsymbol{P^{\beta}})$ (shown in figure 6) since they are multimodal. Solutions $\boldsymbol{x} \in \boldsymbol{X}^{Ut}$ that do not belong to the front $f^{max}(\boldsymbol{X^{Wc}}, \boldsymbol{P^{\alpha}})$ or $f(\boldsymbol{X^{Nom}}, \boldsymbol{p}^0)$ present a better trade-off between optimal and robust performance. In this figure, the reference controllers $\boldsymbol{x}^3 \in \boldsymbol{X}^{Ut}$, $\boldsymbol{x}^2 \in \boldsymbol{X}^{Wc}$, and $\boldsymbol{x}^1 \in \boldsymbol{X}^{Nom}$ are also highlighted.

To visualize another comparison between the performance trend of the controllers $\boldsymbol{X^{Ut}}$, $\boldsymbol{X^{Wc}}$ and $\boldsymbol{X}^{Nom}$ obtained from different optimization approaches, figure 8 shows the system response with the reference controllers highlighted before $\boldsymbol{x}^1 \in \boldsymbol{X}^{Nom}$ (red), $\boldsymbol{x}^2 \in \boldsymbol{X}^{Wc}$ (black), and $\boldsymbol{x}^3 \in \boldsymbol{X}^{Ut}$ (green) under the nominal model $\boldsymbol{p^0}$ for a simulation time of 3300 seconds. This figure shows again

that controller $\boldsymbol{x}^3 \in \boldsymbol{X}^{Ut}$ exhibits a system response with a balanced performance concerning controllers $\boldsymbol{x}^1 \in \boldsymbol{X}^{Nom}$ and $\boldsymbol{x}^2 \in \boldsymbol{X}^{Wc}$ for the outputs $[T_{w_{out}}, T_{w_{in}}]$ and inputs $[u_{T_{wout}}\ u_{T_{win}}]$. On the other hand, figure 9

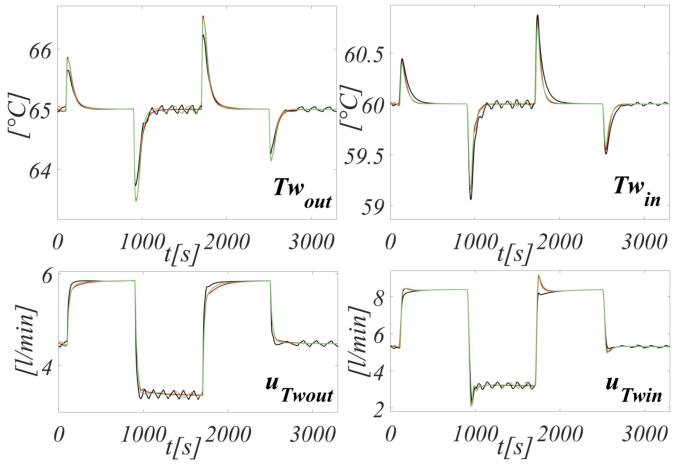

Fig. 8. System response obtained with the controllers $\boldsymbol{x}^1 \in \boldsymbol{X}^{Nom}$ (red), $\boldsymbol{x}^2 \in \boldsymbol{X}^{Wc}$ (black), and $\boldsymbol{x}^3 \in \boldsymbol{X}^{Ut}$ (green) under the nominal model $\boldsymbol{p^0}$.

shows the response envelope of the system for the outputs and inputs obtained by simulating the controllers $\boldsymbol{x}^3 \in \boldsymbol{X}^{Ut}$ (green), $\boldsymbol{x}^2 \in \boldsymbol{X}^{Wc}$ (black), and $\boldsymbol{x}^1 \in \boldsymbol{X}^{Nom}$ (red) under the set of uncertainty models $\boldsymbol{P}^{\alpha}$. The solid and dashed lines represent the upper and lower bounds of each envelope respectively. These bounds exhibit the degradation for each controller under uncertainties. The performance balance in the objective space under the nominal and worst-case scenarios involved in the definition of $\boldsymbol{X}^{Ut}$ causes the solution $\boldsymbol{x}^3 \in \boldsymbol{X}^{Ut}$ to show a tendency to exhibit a degradation range (area bounded by the green upper and lower limits) with lower amplitude.

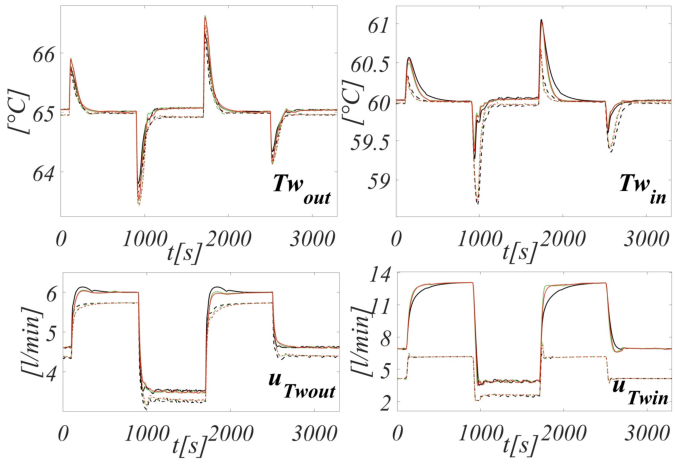

Fig. 9. System response envelope obtained with the controllers $\boldsymbol{x}^1 \in \boldsymbol{X}^{Nom}$ (red), $\boldsymbol{x}^2 \in \boldsymbol{X}^{Wc}$ (black), and $\boldsymbol{x}^3 \in \boldsymbol{X}^{Ut}$ (green) under $\boldsymbol{P}^{\alpha}$. Solid lines indicate upper limits. Discontinuous lines indicate lower limits.

5. CONCLUSIONS

This paper shows the Utopian robust efficiency indicator for tuning a multiloop PID control structure. The application process is the control of several temperatures of a PEMFC system. The design aimed to optimize the system performance in the nominal scenario, the worst-case scenario and the utopian robust efficiency. The analysis of results highlights the utopian robust efficiency as an effective indicator for tuning controllers with a balanced trade-off between optimal and robust performance.

REFERENCES

Ellamla, H.R., Staffell, I., Bujlo, P., Pollet, B.G., and Pasupathi, S. (2015). Current status of fuel cell based combined heat and power systems for residential sector. *Journal of Power Sources*, 293, 312–328.

Gaspar-Cunha, A. and Covas, J.A. (2008). Robustness in multi-objective optimization using evolutionary algorithms. *Computational optimization and applications*, 39, 75–96.

Herrero, J.M., García-Nieto, S., Blasco, X., Romero-García, V., Sánchez-Pérez, J.V., and Garcia-Raffi, L. (2009). Optimization of sonic crystal attenuation properties by ev-moga multiobjective evolutionary algorithm. *Structural and Multidisciplinary Optimization*, 39(2), 203–215.

Ide, J. and Schöbel, A. (2016). Robustness for uncertain multi-objective optimization: a survey and analysis of different concepts. *OR spectrum*, 38(1), 235–271.

Miettinen, K. (2012). *Nonlinear multiobjective optimization (Vol. 12)*. Springer Science & Business Media.

Navarro, S., Herrero, J.M., Blasco, X., and Simarro, R. (2020). Design and experimental validation of the temperature control of a pemfc stack by applying multiobjective optimization. *IEEE Access*, 8, 183324–183343.

Navarro Giménez, S., Herrero Durá, J.M., Blasco Ferragud, F.X., and Simarro Fernández, R. (2019). Control-oriented modeling of the cooling process of a pemfc-based μ -chp system. *IEEE Access*, 7, 95620–95642.

Paenke, I., Branke, J., and Jin, Y. (2006). Efficient search for robust solutions by means of evolutionary algorithms and fitness approximation. *IEEE Transactions on Evolutionary Computation*, 10(4), 405–420.

Pajares, A., Blasco, F.X., Herrero, J.M., and Vicente Salcedo, J. (2020a). Analyzing the nearly optimal solutions in a multi-objective optimization approach for the multivariable nonlinear identification of a pem fuel cell cooling system. *IEEE Access*, 8, 114361–114377.

Pajares, A., Blasco, X., Herrero, J.M., and Simarro, R. (2020b). Multivariable controller design for the cooling system of a pem fuel cell by considering nearly optimal solutions in a multiobjective optimization approach. *Complexity*, 2020.

Shang, C., Huang, X., and You, F. (2017). Data-driven robust optimization based on kernel learning. *Computers & Chemical Engineering*, 106, 464–479.

Veyna, U., Blasco, X., Herrero, J., and Pajares, A. (2023a). Non dominated robust solutions design under a multi-objective optimization approach. applied to robust controllers tuning. *Under review in a JCR journal.*

Veyna, U., Blasco, X., Herrero, J., and Pajares, A. (2023b). Parameter uncertainty modeling for multiobjective robust control design. application to a temperature control system in a proton exchange membrane fuel cell. *Engineering Applications of Artificial Intelligence*, 119, 105758.